“The electrorheological performance of polyaniline-based hybrid particles suspensions in silicone oil: influence of the dispersing medium viscosity”

C. Roman[1], M. García-Morales[1*], S. Goswami[2], A.C. Marques[2] and M.T. Cidade[2]

[1] *Departamento de Ingeniería Química, Centro de Investigación en Tecnología de Productos y Procesos Químicos (Pro2TecS), Campus de “El Carmen”, Universidad de Huelva, 21071, Huelva (SPAIN)*

[2] *Departamento de Ciência dos Materiais, CENIMAT/I3N, Faculdade de Ciências e Tecnologia, Universidade Nova de Lisboa, 2829-516, Caparica (PORTUGAL)*

[*]Author to whom correspondence should be addressed:

Moisés García-Morales, PhD

E-mail: moises.garcia@diq.uhu.es

Phone: +34 959 21 82 07

Fax: +34 959 21 99 83

ABSTRACT

The potential of electrorheological (ER) suspensions based on polarizable particles in simple liquids relies on the particles arrangements which turn their quasi Newtonian behavior into gel-like. However, minor attention has been paid to the effect provoked by the liquid viscosity on the ease of orientation and assembly of the particles. With this aim, a study on the ER behavior, at 25ºC, of 1 wt.% suspensions of polyaniline-based hybrid particles (-graphene or –tungstene oxide) in silicone oil with varying viscosities (20, 50 and 100 cSt) was carried out. The electric field effect was higher for the polyaniline-graphene particles suspension in the less viscous silicone oil. However, two drawbacks were observed: a) higher leakage current flows; and b) reduced reversibility upon the electric field was turned off. The use of silicone oil with higher viscosity solved these issues.

Keywords: Electrorheology; Polyaniline; Graphene; Tungsten oxide; silicone oil; viscosity; smart fluids.

1. Introduction

Smart functional materials have recently gained considerable attention in both scientific and industry community, because they are able to respond to various external stimuli involving temperature, mechanical stress, and electric or magnetic field [1]. Thus, they could be exploited in a multitude of technological applications [2]. Among them, electrorheological (ER) fluids have shown great potential because of their simple mechanics, rapid reversible transition and low power consumption [3-5]. The most common type of ER fluids consists of micron- or submicron-sized polarizable particles homogenously dispersed in an electrically non-conductive liquid. Silicone oil is often used as suspending medium. Upon application of an external electric field their microstructure changes in such a way that a transition from quasi- Newtonian-like behavior to a shear-thinning fluid with yield stress, enhanced shear viscosity and gel-like dynamic shear moduli occurs [4, 5].

Since Winslow [6] first discovered the ER effect, the increasing interest for the high potential of this technology has led to extensive contributions to the soft matter field. Undoubtedly, the ER performance is mainly affected by parameters associated to the dispersed phase, such as dielectric constant, volume fraction, or particle shape and size, variables which have been largely evaluated. In contrast, the influence exerted by the dispersing medium viscosity on the formation of column-like structures upon particle polarization has captured much less attention.

Many advanced materials with various physical and morphological properties have been used as electrically-polarizable particles in ER fluids, including inorganic materials, natural organic compounds, semiconducting or conducting polymers, composites, and novel nanostructured materials with a core-shell structure [4, 7].

Among these materials, conducting polymers have received considerable attention based on their advantages such as a wide range of working temperature, facile variation in conductivity, intrinsic polarizability, low cost and relatively low current density. In particular, polyaniline (PANI) is one of the conducting polymers most frequently used in ER fluids because it meets the above-mentioned list of desirable properties [8-10]. Despite that, both nano/microstructured PANI hybrids have also been developed in order to improve further its limited ER performance.

The hybridization of PANI with carbon materials (e.g. graphene, graphene oxide, CNTs) has revealed beneficial for ER performance, due to the synergistic contribution of the components, which in turn cannot be directly achieved by individual materials [11-13]. Pure graphene is not suitable for ER fluids because of its high conductivity [14]. However, Yin et al. [13] reported the enhanced activity of 2D PANI-decorated graphene sheets, as compared to the traditional granular PANI.

Recently, various metal oxides have opened up opportunities in the development of electrochromic devices. Among them, tungsten trioxide (WO_3) has drawn considerable attention for its unique electronic/protonic conductivity and its high coloration efficiency. Since the first electrochromic study on WO_3 reported by Deb [15] this metal oxide has been further proposed as an ideal candidate for a number of applications: chemical sensors, photocatalysis and “smart windows” [16, 17]; and even as an anode material for lithium ion batteries due to its large theoretical capacity, low cost, high melting temperature and mechanical stability [18, 19].

The combination of inorganic and organic materials yields hybrid particles on which the inorganic moiety assures mechanical strength while the organic part delivers bonding between the inorganic components. The development of hybrid materials based on conducting conjugated polymers, like PANI, and transition metal oxides, which combine

the advantages of both materials and exhibit enhanced electrochromic properties, has been the focus of extensive investigation. In particular, substantial progress in the performance of PANI/WO_3 nanocomposites has been reported [20-21]. However, to the best of our knowledge, there is no published literature on their electrorheological properties. Hence, PANI/WO_3 nanocomposites require further study in terms of their capacity to change the rheological behavior of suspending Newtonian media when subjected to electric fields perpendicular to the flow direction.

Because of their high ER performance, nanometer scale, non-abrasive PANI moiety and good dispersibility in silicone oil, PANI-Graphene or PANI-WO_3 particles might find application in the development of smart lubricants, which are lately attracting much interest. According to the model Stribeck curve for the friction coefficient, there exist three lubrication regimes (boundary, mixed and hydrodynamic) depending on the gap between the lubricated surfaces [22]. In that sense, friction and wear can be minimized by accommodating, through electric potential control, the lubricant viscosity to local lubricating regimes and temperatures.

Based on the comments above, this article presents a comparative evaluation of the ER performance, at 25ºC, of PANI-Graphene (polymer-carbon hybrid) and PANI-WO_3 (polymer-inorganic hybrid) composite particles in silicone oil. The effect of the silicone oil viscosity has also been addressed. It was found that PANI-Graphene particles are more efficient. However, their combination with low viscosity silicone oil presented some limitations.

2. Experimental

2.1. Particles syntheses

The composites of polyaniline with graphene and WO_3 were prepared via simple chemical oxidative polymerization. At first, the inorganic components i.e. graphene and WO_3 were synthesized separately. Then, those were embedded into the polymeric matrix/backbone of PANI.

The graphene powder was produced following Lin et al. [23] with few modifications, by total ablation of a 75 μm polyimide sheet (Kapton HN, Goodfellow) through laser irradiation with a CO_2 10.6 μm infrared pulsed laser cutting machine (VLS 3.50 Universal Laser Systems, USA) with 40 W power at 0.127 m/s speed. Such irradiation of the commercial polyimide film by a CO_2 infrared laser under ambient conditions converted the film into porous graphene.

On the other hand, the WO_3 particles were synthesized by hydrothermal route following Santos et al. [24]. Typical method followed: 0.4 g of $Na_2WO_4 \cdot 2H_2O$ (Fluka, 99%) was dissolved in 8 g of deionized water with 0.15 g of NaCl (Panreac, 99.5%) (as structure directing agent) and then acidified with 1 g of 6 M HCl solution (Fluka, 37%). The mixture was transferred to a 23 mL PTFE chamber, set inside a stainless-steel autoclave (4745 general purpose vessel, Parr) and installed in an oven (L3/11/B170, Nabertherm). The reaction temperature was set at 180 °C for 1 h followed by a cooling period to room temperature inside the oven. The product material was separated out by centrifugation at 3000 rpm for 2 min (F140, Focus instruments) and washed three times with water. As-synthesized WO_3 nanoparticles were finally collected after drying in the oven (TK4067, EHRET) at 60 °C for at least 8 h.

For incorporating these inorganic parts inside PANI a typical wet-chemical route was followed: First of all, the inorganic particles (2 mg) were well dispersed in 10 mL ethanol-water solution by mechanical stirring for 24 h; then embedded into PANI by simple chemical oxidative polymerization of aniline monomer (Sigma-Aldrich, ≥99.5%) at 0˚C

(ice bath) in presence of ammonium persulfate as oxidant (APS, Sigma-Aldrich ≥98.0%), hydrochloric acid as dopant (HCl, Sigma-Aldrich, 37%) and 10-camphorsulfonic acid as structure directing agent (CSA, Sigma-Aldrich, 99%). Aniline was drop by drop added to 20 mL of ethanol-water solution followed by mixing of CSA (aniline: CSA = 1M:0.25M) and then cooled at 0 ˚C for 20 min. Then, APS and HCl (APS: HCl: Aniline = 1:1:1) were added to the pre-cooled (0˚C) 10 mL inorganic particle dispersion. Afterwards, it was dropwise added to the pre-cooled monomer solution with 15 s shaking. The reaction chamber was maintained at 0˚C for 2 h without stirring. The greenish black precipitate is separated by filtration and washed thoroughly with excess de-ionized water and methanol to remove unreacted monomer and oligomers. Final materials were collected after vacuum drying at 60 ˚C for next 24 h.

2.2. Preparation and rheological characterization of ER suspensions

ER fluids were prepared by dispersing the above hybrid particles (PANI-Graphene or PANI-WO_3) in silicone oils with varying viscosities, at the fixed concentration of 1 wt.%. Dispersion was carried out by sonication, for 30 minutes. In order to ensure the dispersed state of the suspensions being characterized, sonication was again conducted for 10 minutes before the rheological tests. Silicone oils of three different kinematic viscosities of 20, 50 and 100 cSt, and densities between 0.950 and 0.966 $g \cdot cm^{-3}$, at 25ºC, were used. All these polydimethylsiloxane fluids, commercialized as PSF-20, -50 and -100 cSt Pure Silicone Fluids, were purchased from Clearco Products Co. Inc., USA. They will be referred to hereinafter as 20, 50 or 100 cSt silicone oils.

Rheological tests were performed with a controlled stress rheometer, Bohlin Gemini HR^{nano} (Malvern, Worcestershire, UK). The rheometer was equipped with a special cell for ER characterization and a high current voltage generator, SPELLMAN SL150,

(Spellman High Voltage Electronics Corporation, USA). DC electric fields up to 2 $kV \cdot mm^{-1}$, when possible, perpendicular to the flow direction were applied. It is worth noting that the generator reaches saturation when a leakage current of 15 mA is attained. In order to assure the equilibrium structure of ER fluids, the applied voltage was maintained for at least 3 minutes before running the tests. Plate-plate geometry, with 40-mm diameter and 500-μm gap between upper and bottom plates were used. The rotating upper plate is accessorized with a reservoir filled with a conductive aqueous solution such that the voltage applied by the electrode is not in direct contact with the metal.

The rheological characterization, at 25ºC, consisted in steady shear viscous flow tests and dynamic shear frequency sweep tests in linear regime. Isothermal tests were developed in the absence of electric field (reference value) and under electric fields of varying intensities. Viscous flow tests were conducted over a shear rate interval between 0.01 and 300 s^{-1}. In order to erase influence of previous measurements, the ER suspensions were subjected to a pre-shear at a constant shear rate of 1 s^{-1} for 60 s, followed by equilibration for 300 s, before running a test. As for the characterization on dynamic shear mode, preliminary strain sweep tests, at the frequency 1 Hz, were performed in order to determine the strain range over which the ER fluids exhibit linear viscoelastic (LVE) response. Then, their linear viscoelastic behavior was evaluated through dynamic shear frequency sweeps, between 0.03 and 100 rad/s, at fixed strain values within the LVE range.

In order to ensure the accuracy of the results obtained, each ER fluid was tested at least three times. Hence, the results shown are the average value of different replicates.

3. Results and discussion

3.1. Morphological and structural characterization of the particles

The morphological characterization of as-synthesized materials was performed by the scanning electron microscopy (SEM, Auriga SEM-FIB, Zeiss) as depicted in Figure 1. The graphene synthesized via laser ablation technique is porous in nature as shown in Figure 1A and the composite as formed with PANI is presented in Figure 1B. The WO_3 particles before incorporating within the PANI matrix is shown in Figure 1C and the composite with PANI is as presented in Figure 1D. Both of the composites have mixed structures in their morphology, but that with WO_3 has more prominent fibre-like structures along with the other particulates. Also, it can be concluded from the SEM images that the over-all aspect ratio is higher for the PANI-WO_3 composite.

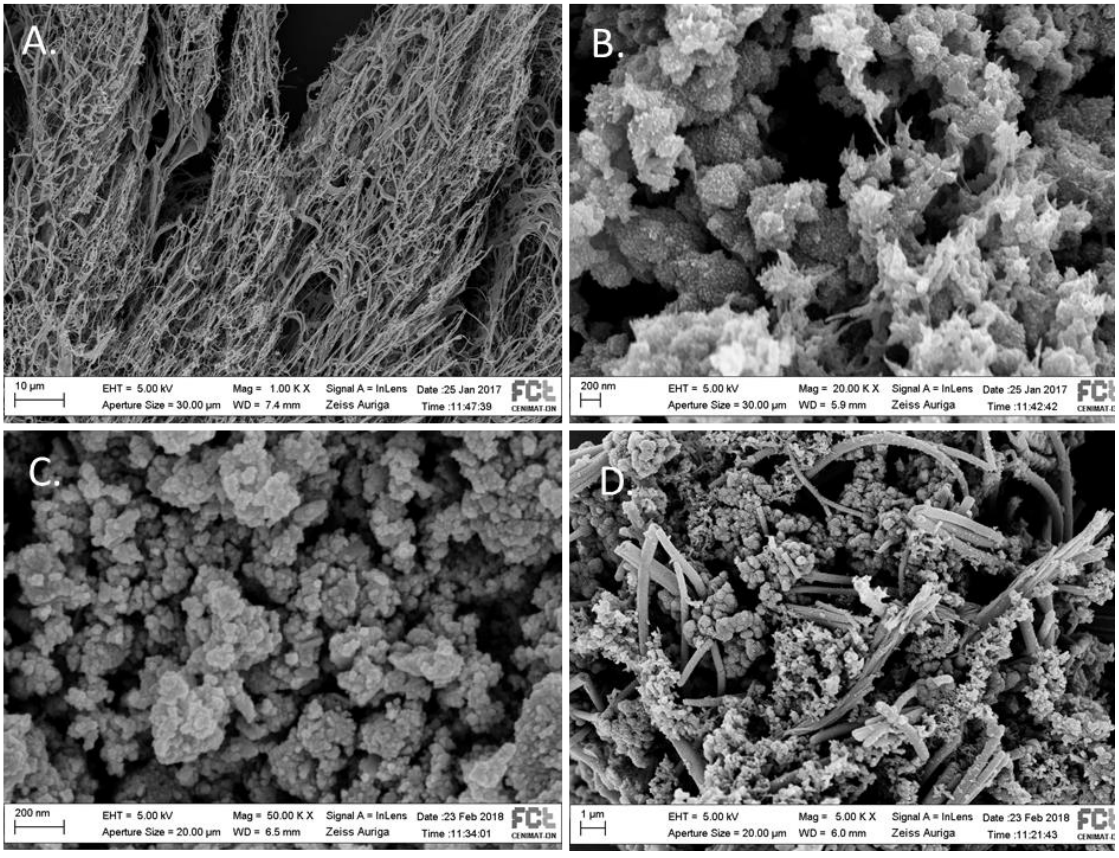

Figure 1. Graphene prepared by laser ablation technique (A); PANI-Graphene composite (B); WO_3 particles (C); and PANI-WO_3 composite (D).

Also, elemental analysis of the particles was carried out by Energy-Dispersive X-ray Spectroscopy (EDS). The EDS spectrum was acquired using an Oxford X-Max 150

detector inside the same Zeiss Auriga Crossbeam platform. The initial idea was to obtain a confirmation of the hybrid structure formation, by monitoring the intensity of the elemental mapping over the samples. The mapping as presented in Figure 2 well confirms the formation of the PANI-WO_3 composite; though in the SEM image the morphology was looking more like simple mixtures, but from the EDS spectra with mapping it is now more evident that the WO_3 particles are all through incorporated within PANI to form the composite.

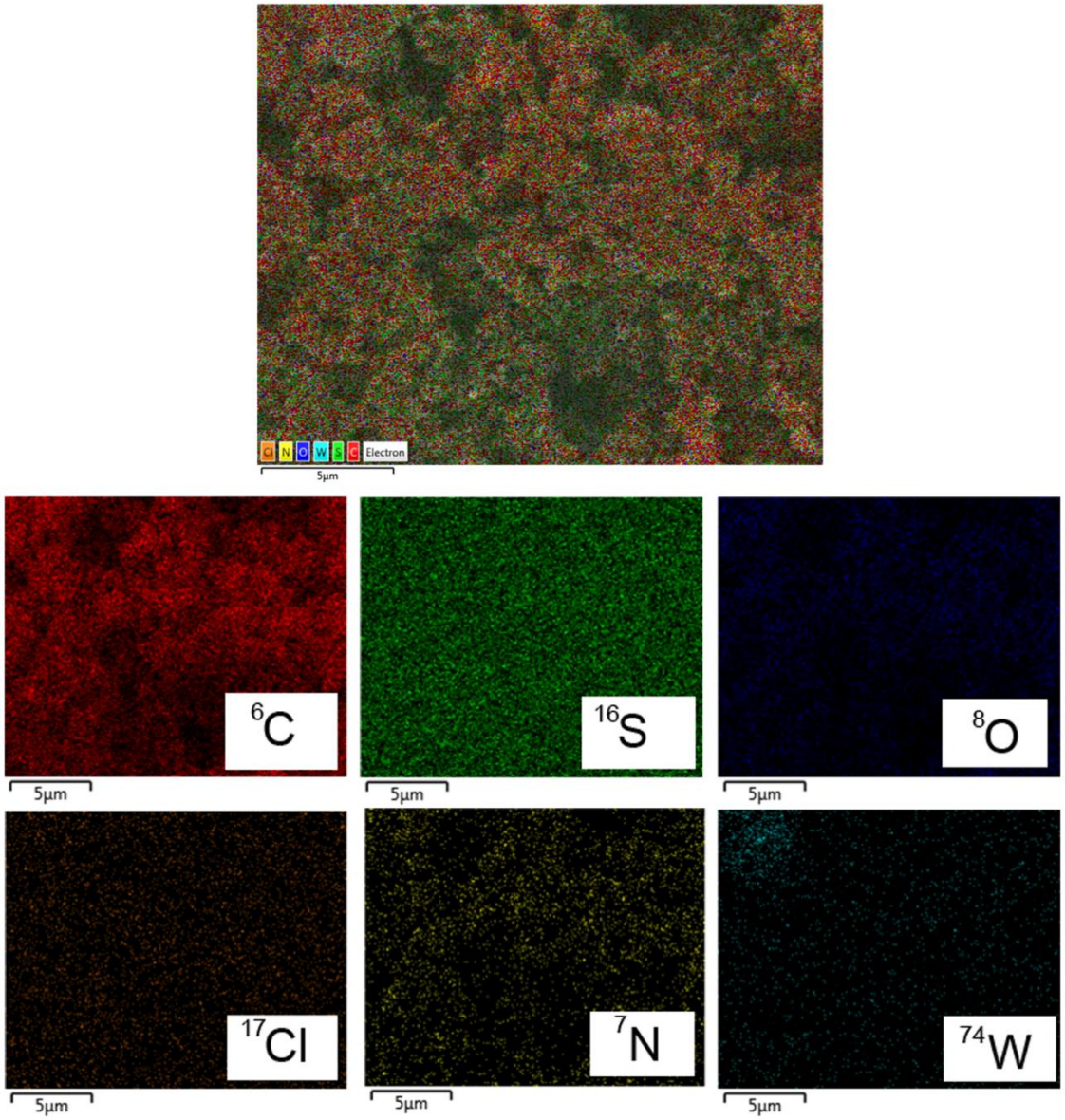

Figure 2. EDS analysis with mapping of elements present in as-synthesized PANI-WO_3 composite. Each element has different individual colors merged and specified in the layered image (top).

However, in case of PANI-Graphene (Figure 3), the EDS analysis is not giving any obvious proof of the state/incorporation of graphene within PANI because both of them have “C” as the main elemental part. Moreover, in both the composites, there are traces of “S” and “Cl” in the elemental mapping which support the fact of formation of doped PANI in these cases. The contributions of “N” and “O” are coming from PANI and atmosphere.

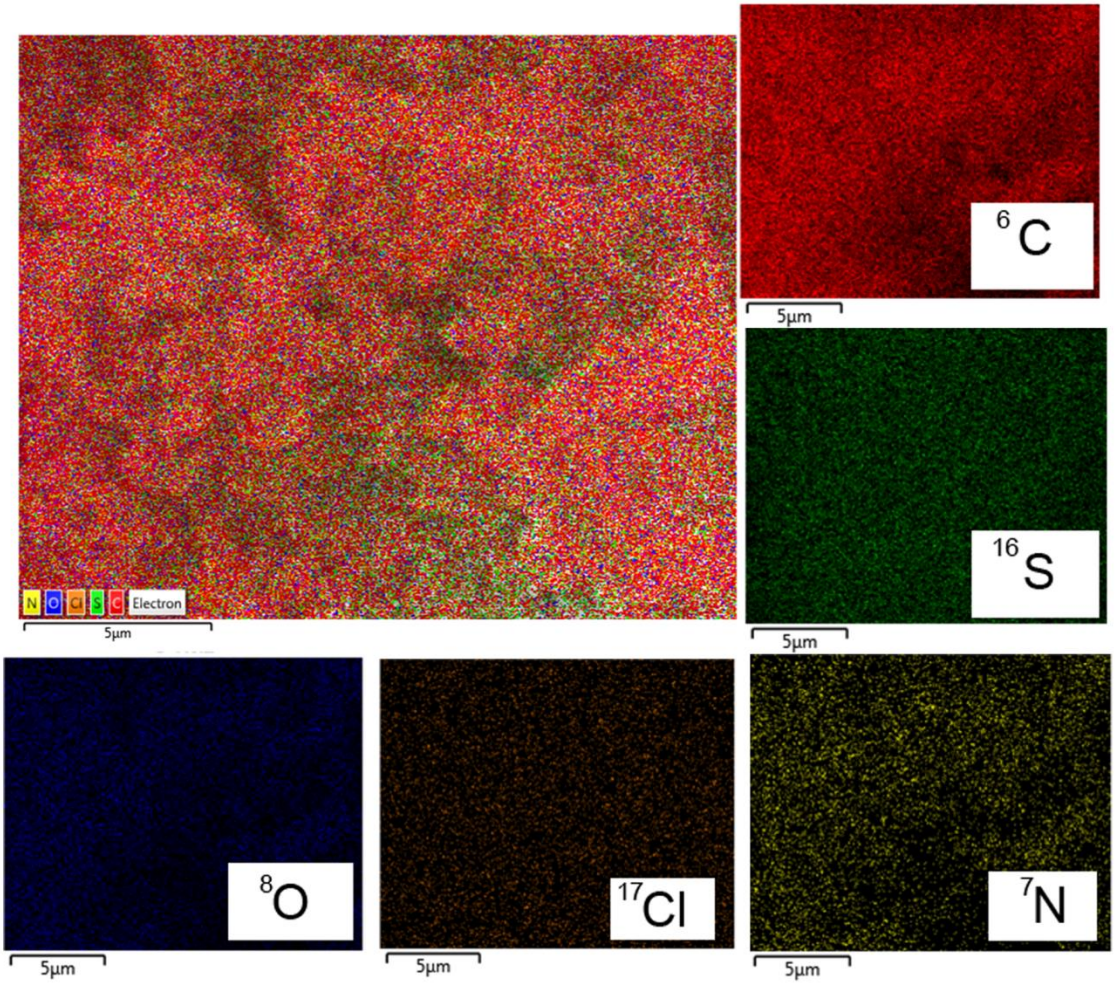

Figure 3. EDS analysis with mapping of elements present in as-synthesized PANI-Graphene composite. Each element has different individual colors merged and specified in the layered image (top left).

For further study of chemical structures of the composites, Raman spectroscopy was carried out by Renishaw Qontor InVia Raman microscope. The Raman measurements are

performed with the excitation laser line of 633 nm using 10% of the max. laser power (50 mW) and exposure time 1s for each 5 accumulations. The Raman spectra as obtained for both the composites are depicted in Figure 4, which also confirm the chemical identities of the samples as follows.

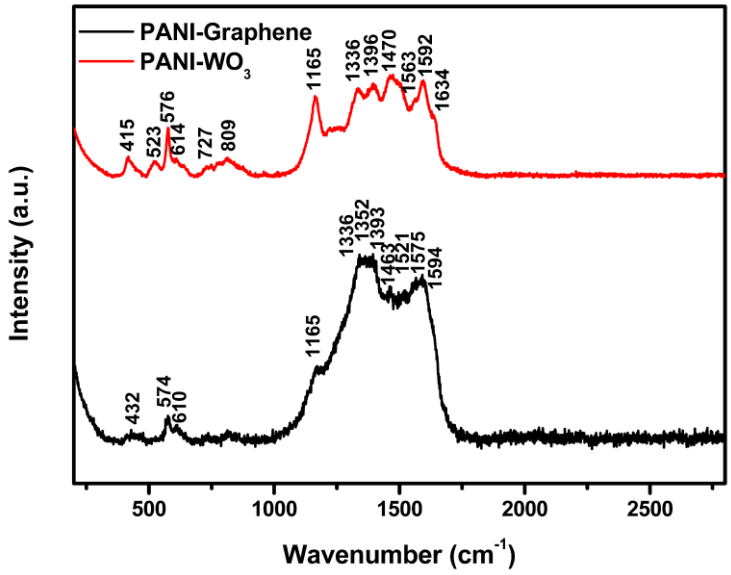

Figure 4. Typical Raman spectra of as-synthesized PANI-WO_3 and PANI-Graphene composites.

The typical Raman spectrum of PANI-WO_3 has shown its characteristic bands around 415, 523, 576, 614, 727, 809, 1165, 1336, 1396, 1470, 1563, 1592 and 1634 cm^{-1}. Among these, the bands at 727 and 809 cm^{-1} corresponds to the O─W─O stretching modes, thus confirming also the presence of WO_3 within the composite [25, 26]. The rest of the bands are attributed to PANI: For example, bands at 1563, 1592 and 1634 cm^{-1} are due to the C═C stretching modes in the Quinoid or Benzenoid rings; the bands starting from 1165 to 1470 cm^{-1} are ascribed to different types of C─N stretching modes (amines, imines, polarons, bipolarons); the band at 415 cm^{-1} is assigned to C─H deformation whereas other bands at 523, 576 and 614 cm^{-1} are related to benzene deformations of variously substituted aromatic rings; which match well with those reported previously [25, 27, 28].

However, very small shifts are present due to the tight incorporation of the inorganic particles within the polymer backbone introducing some stretching vibrations effect. For PANI-Graphene composite, the Raman spectrum showed the presence of typical characteristic bands of Graphene at around 1352 cm^{-1} (D-band, attributed to the defects and edge areas) and 1575 cm^{-1} (G-band, attributed to the vibration of sp^2-hybridized carbon); though the bands are broad and overlapped in some part with the characteristic peaks of PANI, which suggests strong interactions between the N-atoms in PANI and the π-electrons in Graphene systems. Also, the absence of 2D-band at 2710 cm^{-1} corresponds to the fact of Graphene existing within PANI matrix in few layers [29]. Furthermore, these Raman spectra are also revealing that in both the cases the interaction and overlapping of the π-conjugated systems have affected each individual component within the composites.

3.2. Rheological characterization of ER fluids

The ER behavior of 1 wt.% PANI-Graphene particles suspensions in silicone oil, at 25ºC, was studied. Figures 5A and 5B present a comparative evaluation of the effect of the silicone oil viscosity, by using oils with 100 and 20 cSt, respectively.

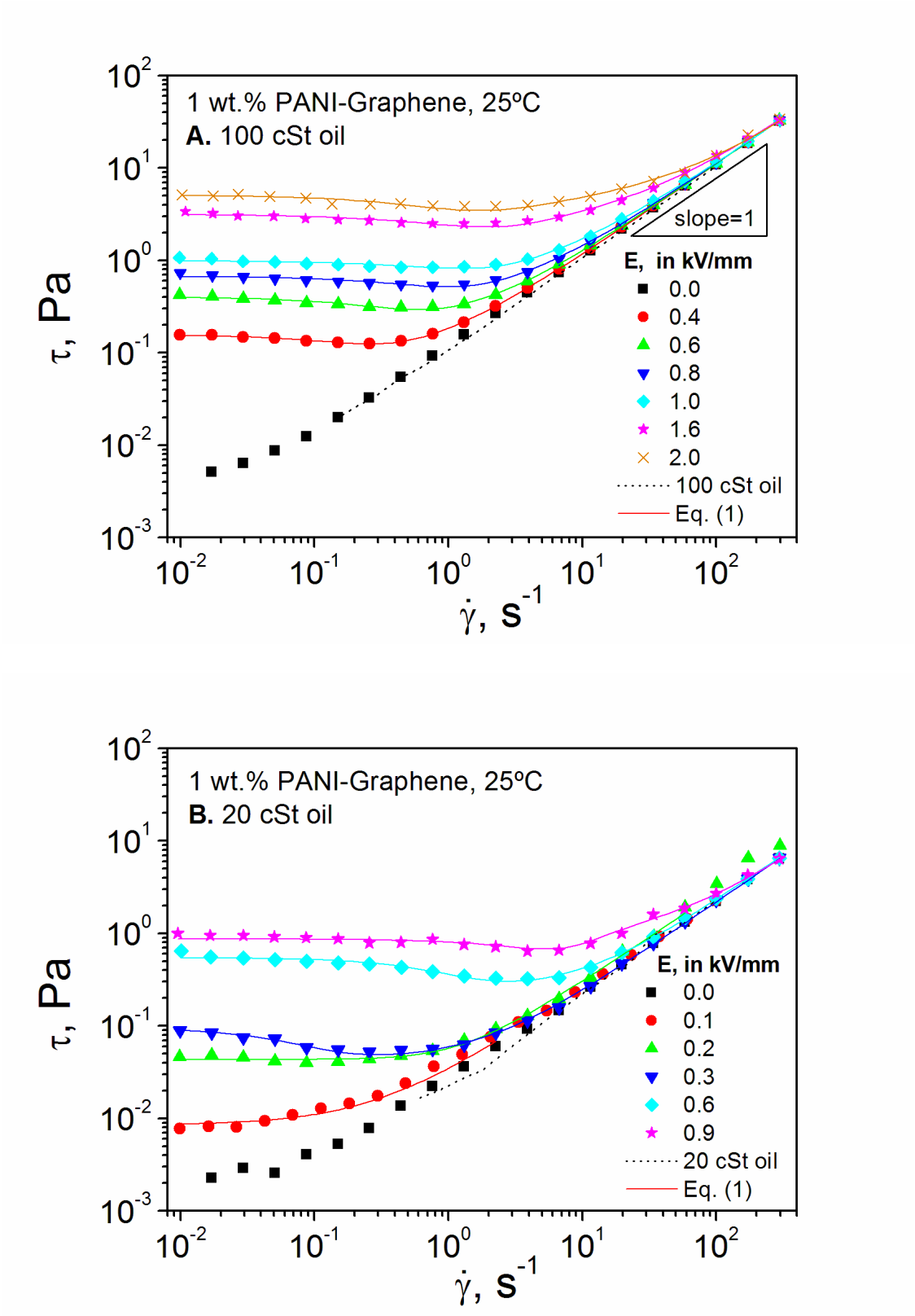

Figure 5. Evolution of shear stress with shear rate, at 25ºC, as a function of the electric field for 1 wt.% PANI-Graphene suspensions in silicone oil with 100 cSt (A) and 20 cSt (B).

In the absence of electric field, the ER suspensions exhibit, at shear rates higher than 0.1 s^{-1}, the viscous flow behavior which characterizes the Newtonians fluids. Thus, in a double-log plot of shear stress versus shear rate, the relationship between these parameters is a straight line with a slope of 1. Below 0.1 s^{-1}, some shear-thinning behavior was observed. At the low concentration of 1 wt.%, the addition of PANI-Graphene particles to silicone oils with varying viscosities only produces minor changes on their viscous flow behavior if no electric field is applied. However, under the effect of an electric field, the viscous flow behavior of the above suspensions changes significantly. A yield stress, which increases with the electric field intensity, has to be overcome before the flow commences and the material behaves like a Newtonian fluid. Such a yield stress arises as a consequence of the columnar structures formed due to the interaction between polarized particles oriented according to an electric field perpendicular to the shear direction [4]. Traditionally, the viscous flow behavior of fluids with yield stress, referred to as "viscoplastic" fluids, has been fairly well represented by the Bingham equation [30], with a constant value of yield stress. However, as previously reported for other ER suspensions, Figures 5A and 5B show a first region with a constant value of yield stress (termed "static" yield stress) which is followed by a minimum before the material starts to flow and the shear stress evolution with shear rate is that for a Newtonian fluid. As opposed to standard viscoplastic fluids, ER suspensions under the effect of an electric field present the capacity to re-establish the columnar structures broken by low shearing, extending the shear range interval over which no flow occurs. Under more severe shear conditions, the rate of destruction is higher than the rate of formation. Hence, the broken structures are not balanced by the healing capacity of the ER suspension, and the yield stress presents a minimum before the flow eventually starts. As shown in Figures 5A and 5B, for base silicone oils with 100 and 20 cSt, respectively, Equation (1) is able to

reproduce in detail the viscous flow behavior of the 1 wt.% PANI-Graphene suspensions studied. This equation, reported by Seo et al. [31] and based on a former model proposed by Papanastasiou, is expressed as:

$$\tau(\dot{\gamma}) = \tau_{sy} \cdot \left(1 - \frac{1 - \exp(-a \cdot \dot{\gamma})}{1 + (a \cdot \dot{\gamma})^{\alpha}} \right) + \eta_{\infty} \cdot \dot{\gamma} \qquad (1)$$

where τ_{sy} is the static yield stress; α is an exponent related to the shear thinning degree; **a** is a time constant defined as the inverse of shear rate at which flow starts; and η_{∞} is the high-shear-rate Newtonian viscosity. As observed in Figures 5A and 5B, the minimum in the yield stress shifts to higher shear rate values with increasing the electric field intensity, because higher fields bring about more powerful healing capacity of the ER suspension. It is noteworthy that in the case of the 20 cSt silicone oil suspension the electric field was limited to 0.9 kV/mm. Beyond this value, the leakage current exceeded the maximum value measured by the electric field generator, 15 mA. Conversely, it was possible to get up to 2.0 kV/mm in the 100 cSt silicone oil suspension and still remain far from the above maximum value. The formation of ER structures consists in two stages: particle electric polarization and arrangement into aligned assemblies. Whilst the ease of dipole formation is related to the electric field magnitude and the particle susceptibility, their arrangement is strongly dependent on the dispersing medium viscosity. Hence, the arrangement results less efficient in a medium which offers more resistance to orientation and organization, that is, with higher viscosity [32]. In consequence, we hypothesize that hybrid graphene-based particles would orientate more easily in silicone oil with low viscosity. Similar to, for example, polymer-based nanocomposites containing MWCNTs, electron transfer via tunneling can occur between graphene particles in contact or sufficiently close to each other [33]. This might explain the resulting current flow at very low values of electric field. However, a much higher degree of particles assembling could only be confirmed

by microscope visualization of the pattern. Hence, further study on this aspect is still required.

Previous results were plotted in the form of steady shear viscosity curves, in Figures 6A and 6B.

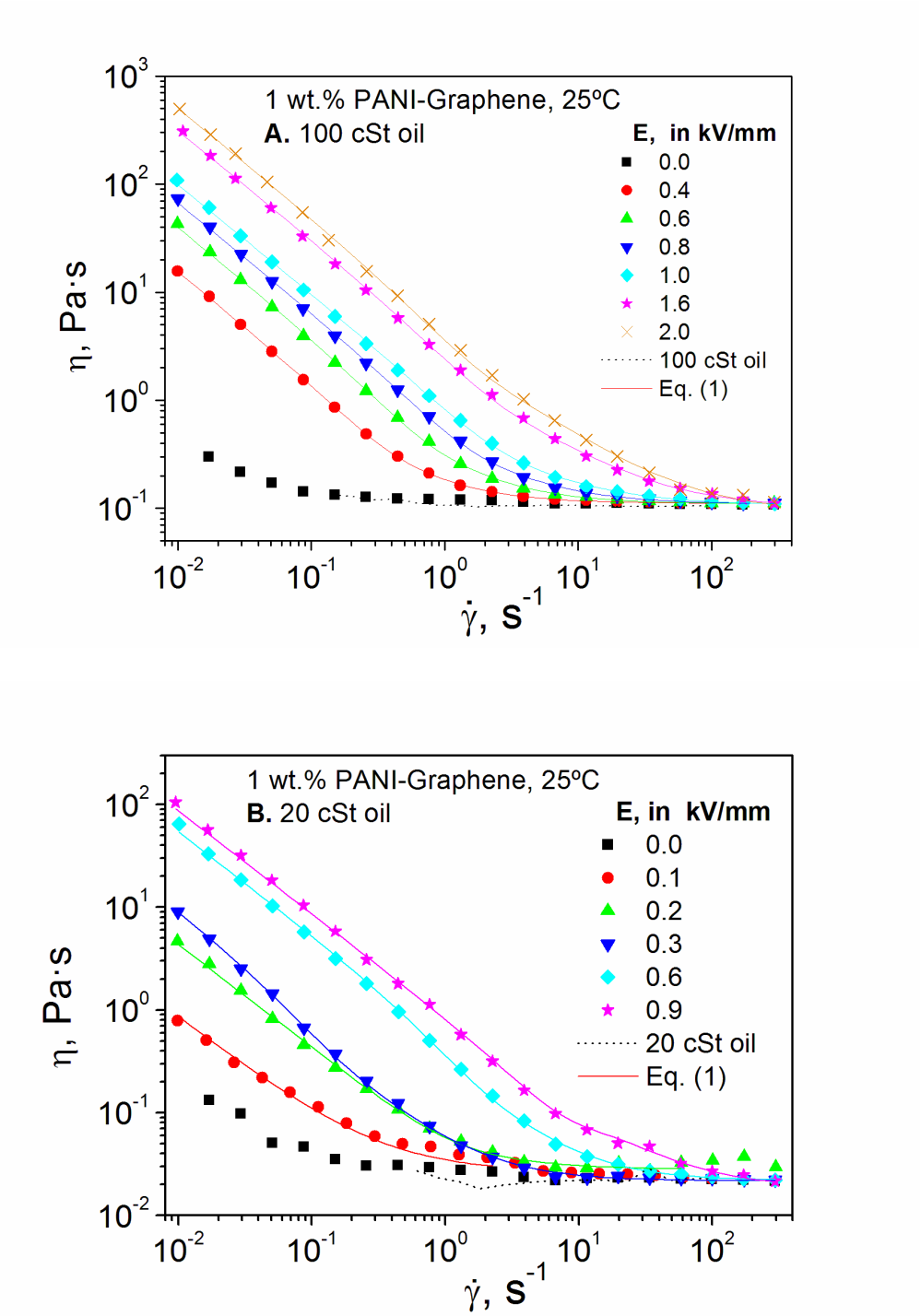

Figure 6. Steady shear viscosity curves, at 25ºC, as a function of the electric field for 1 wt.% PANI-Graphene suspensions in silicone oil with 100 cSt (A) and 20 cSt (B).

If no electric field is applied, the 1 wt.% PANI-Graphene suspensions behave as nearly Newtonian fluids with constant viscosities of 100 and 20 mPa·s, at shear rates higher than 0.1 s^{-1}, in Figures 6A and 6B, respectively. At the low particle content studied, the viscous flow behavior of the base oil undergoes minor changes, as previously discussed. With regard to the electrorheological effect provoked by an electric field, the evolution of the steady shear viscosity with shear rate, at 25ºC, is characterized by a "power-law" shear thinning decay, followed by a transition zone before the high-shear-rate Newtonian viscosity, η_∞, is attained. The power-law interval corresponds to a situation in which the shear rate imposed is not high enough so as to overcome the resistance to flow opposed by the columnar structures arisen with application of electric field. Consequently, the higher the electric field intensity, the higher the yield stress associated to the resulting structure and so the low-shear-rate viscosity. As shear rate is raised, the viscosity measured results from a balance between the local shear acting on the particles (hydrodynamic forces) which rupture the structures, and the electrostatic interactions among the polarized particles which tend to re-establish them. Eventually, at very high shear rates, the complete de-assembling of polarized particles turns the behavior into Newtonian (characterized by η_∞). Furthermore, not only the viscosity but also the current intensity which passes through the sample underwent a marked decay with increasing the shear rate. Logically, if the continuous structures which connect bottom and upper plates break, the electrical resistance increases. Based on that, Figures 6A and 6B demonstrate that for the same silicone oil, the higher the electric field applied, the higher the shear rate for the ER fluid to return to the zero-field viscosity. More interestingly, Figures 6A and 6B also reveal that under the same electric field, the lower the oil viscosity, the higher the

above mentioned critical shear rate. This outcome can be well explained in terms of the dimensionless Mason number, Mn, which is expressed as:

$$Mn = \frac{\eta_C \cdot \dot{\gamma}}{2 \cdot \varepsilon_0 \cdot \varepsilon_C \cdot (\beta \cdot E)^2} \quad (2)$$

where η_C is the continuous phase viscosity; $\beta=(\varepsilon_P-\varepsilon_C)/(\varepsilon_P+2\cdot\varepsilon_C)$ is the dielectric constant mismatch between the particle and medium; ε_0, ε_P and ε_C are the dielectric constants for free space, particle and continuous phase, respectively; and **E** is the electric field applied. There exists a critical value of Mason number above which particles aggregation no longer takes place and the suspension viscosity remains as η_∞. Such a critical value depends on both particle concentration and type [34].

In Figures 6A and 6B, which only display results for a single particle type (PANI-Graphene) and concentration (1 wt.%), the effect of the medium viscosity can be compared with no need of further handling. So, at a certain value of E, the silicone oil with lower viscosity, 20 cSt oil, delays the Newtonian region to higher shear rates values, if compared to the 100 cSt oil.

The evolution of the static yield stress, at 25ºC, with the electric field intensity for the above 1 wt.% PANI-Graphene suspensions is presented in Figure 7, as a function of the oil viscosity.

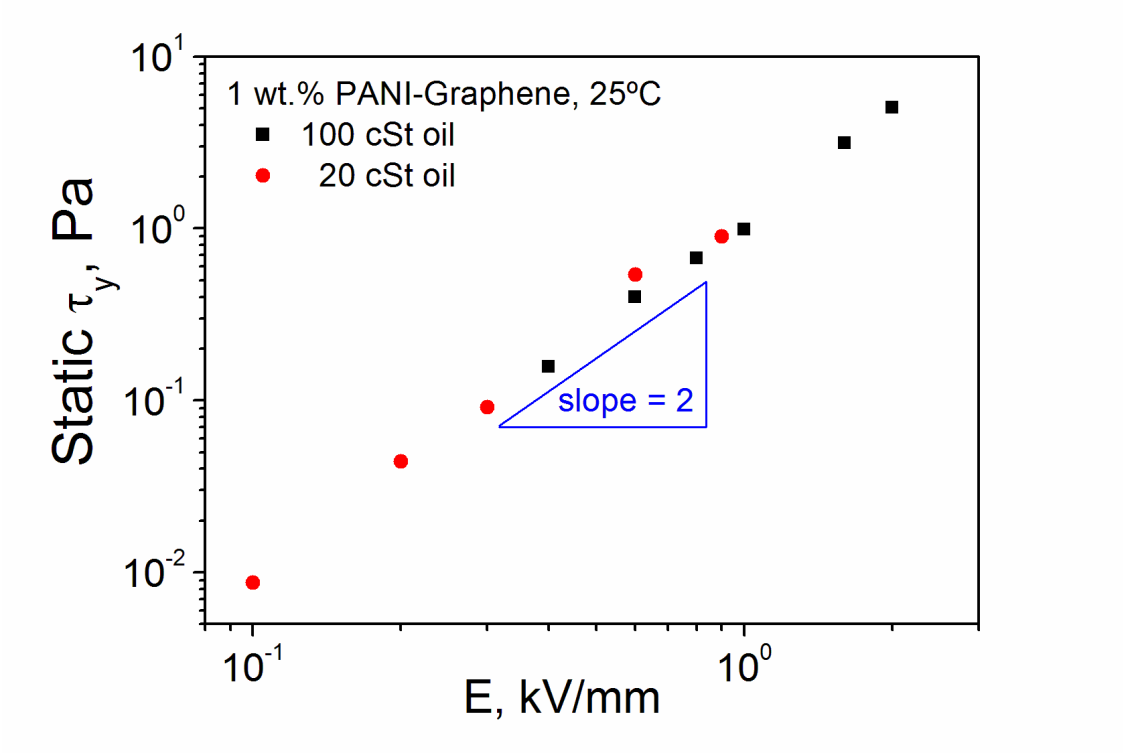

Figure 7. Electric field dependence of the static yield stress, at 25ºC, for 1 wt.% PANI-Graphene suspensions in silicone oil with 100 and 20 cSt.

Both data sets best fit a straight line with a slope of approximately 2 in a double-log representation. It means that these variables follow a scaling law where the yield stress varies as a second power of the electric field, according to Equation (3) below:

$$\tau_{sy}(E) = a \cdot E^{b} \quad (3)$$

with **b** being approximately 2, as derived from the polarization model. According to this model reported elsewhere [4], the strength of the interaction between two polarized particles in a Newtonian fluid (the origin of the yield stress) is mainly attributed to the dielectric constant mismatch between particle and medium, but is also influenced by the particle microstructure. Hence, parameters **a** and **b** are affected by all these variables [8, 9, 35].

The ER performance of two suspensions of a second hybrid particle, made up of polyaniline and tungsten oxide, in the previous 100 and 20 cSt silicone oils was also

assessed and compared with the graphene particles, under the same temperature (25ºC) and concentration (1 wt.%). Some differences in the viscous flow behavior of the 100 cSt oil suspensions were found.

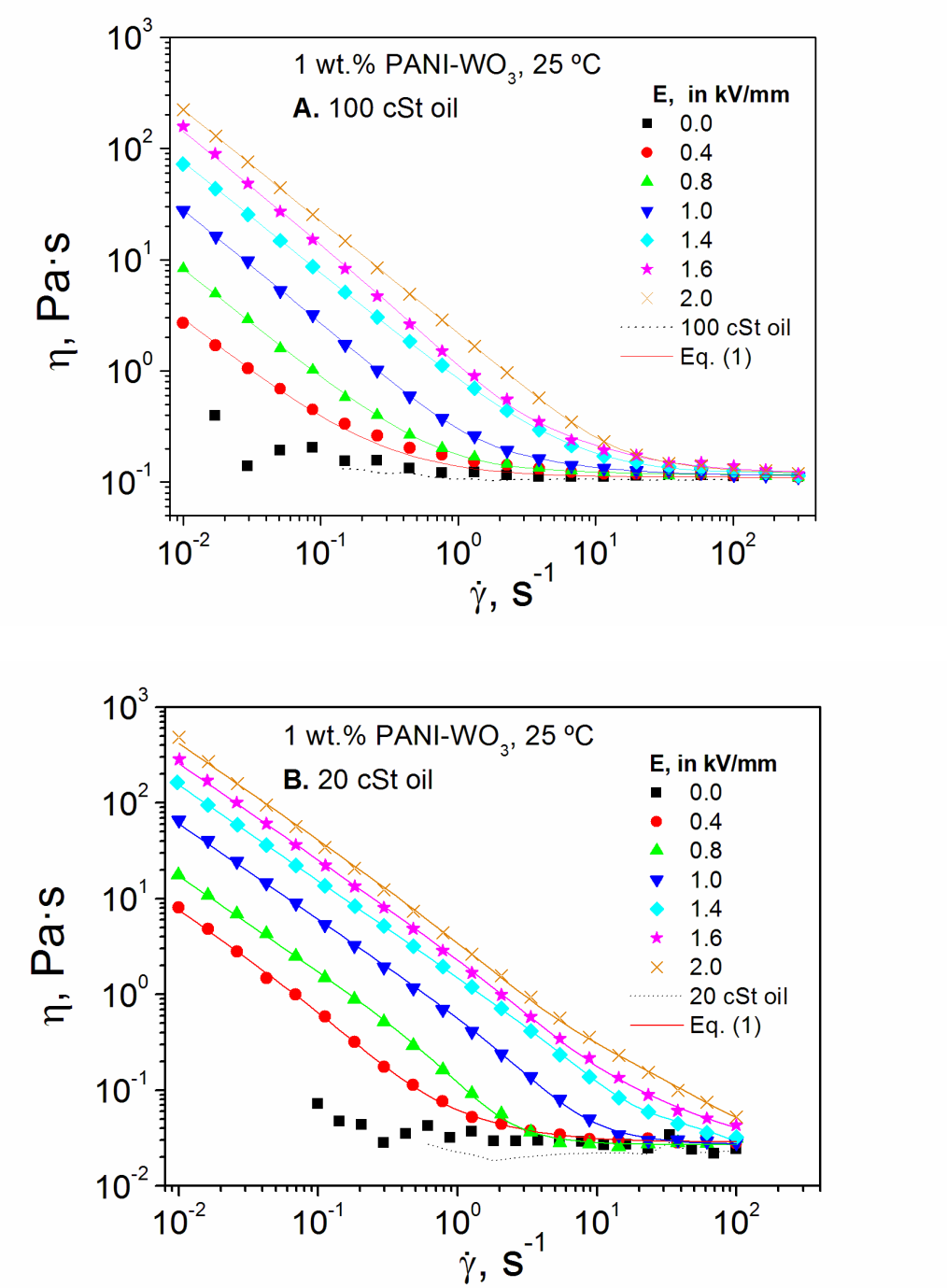

Figure 8. Steady shear viscosity curves, at 25ºC, as a function of the electric field for 1 wt.% PANI-WO_3 suspensions in silicone oil with 100 cSt (A) and 20 cSt (B).

A comparative evaluation of Figures 6A and 8A allows concluding on the stronger ER effect of the PANI-graphene particles, if compared to the tungsten oxide particle. In that sense, Goswami et al. [8] concluded, for polyaniline-vanadium oxide nanostructures suspended in silicone oil, that larger aspect ratios yielded higher ER effect. As concluded from the SEM images in Figure 1, the over-all aspect ratio is higher for the PANI-WO_3 composite. However, other more influencing parameters need to be considered when different particles are compared. The pristine doped PANI moiety presented a conductivity of around 3 S/m. As pristine graphene is highly conductive (10^5 S/m) and pristine WO_3 is non-conductive, the result is a PANI-Graphene nanocomposite with much higher conductivity than the PANI-WO_3 nanocomposite (19.48 S/m and 0.22 S/m, respectively). In consequence, the contribution to the ER activity of the highly conductive PANI-Graphene particle is much more significant than the fibre-like PANI-WO_3 particle. Thus, for the same initial viscosity of 100 mPa·s, at 0.1 s^{-1}, the viscosity values corresponding to an electric field of 2 kV/mm were 50 and 22 Pa·s for the PANI-Graphene and PANI-WO_3 suspensions, respectively. Moreover, in the case of the most electrorheologically favored particle, PANI-Graphene, a higher shear rate was necessary for the hydrodynamic forces to counterbalance the electrostatic interactions and turn the suspension behavior into Newtonian. For example, for an electric field of 2 kV/mm, the shear rate values for the suspension viscosity to drop down to 200 mPa·s (twice the Newtonian viscosity, η_∞) were 15 and 43 s^{-1} for PANI-WO_3 and PANI-Graphene, respectively. Much more remarkable outcomes were found by comparing the ER viscous flow behavior of the two suspensions based on 20 cSt silicone oil, in Figures 6B and 8B. In contrast to the 1 wt.% PANI-Graphene suspension, it was possible to reach an electric field of 2 kV/mm when the 1 wt.% PANI-WO_3 suspension was tested. Again, the above result suggests a higher electric susceptibility for the PANI-Graphene particle.

Remarkable electron mobility in graphene might be behind the higher leakage current observed. As previously reported, the PANI-Graphene nanocomposite exhibits much higher conductivity than the PANI-WO_3 nanocomposite. Finally, with regard to the influence of silicone oil viscosity on the 1 wt.% PANI-WO_3 suspensions, it is worth highlighting again the more remarkable ER effect on a less viscous dispersing medium. This statement is corroborated in Figure 8B by the fact that at a shear rate value as high as 100 s^{-1} and electric field of 2 kV/mm, the suspension is still far from reaching the high-shear-rate Newtonian plateau region. Furthermore, for the above electric field, the relative increase in viscosity is higher in 20 cSt oil than in 100 cSt oil, as observed from Figures 8B and 8A, respectively.

With a view to its practical application, a performance-related parameter termed "efficiency" was estimated, at 25ºC, as follows:

$$Efficiency = \left. \frac{\tau_y(E) - \tau_0}{\tau_0} \right|_{\dot{\gamma}=0.1 s^{-1}} \qquad (4)$$

where τ_0 and $\tau_y(E)$ are the values of shear stress under no electric field and varying electric fields, respectively, at an arbitrarily chosen low shear rate value of 0.1 s^{-1} in Figures 6 and 8. Evolution of efficiency with electric field up to 2 kV/mm, when possible, in a double-log plot is shown in Figure 9.

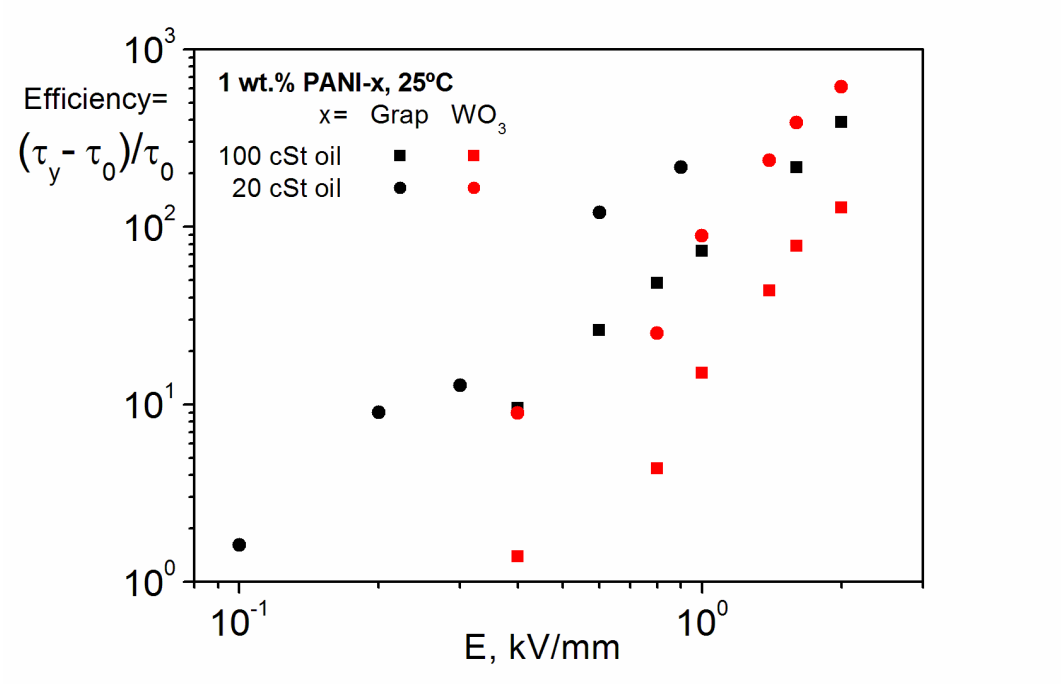

Figure 9. Evolution of the efficiency, in terms of relative increase in shear stress at 0.1 s^{-1} and 25ºC, with electric field for 1 wt. PANI-x (x: Graphene or WO_3) suspensions in silicone oil with 100 and 20 cSt.

Based on these results, we conclude that our graphene-based suspensions exhibit a greater ER performance in terms of the viscosity gain relative to the zero electric field viscosity. A less viscous silicone oil enhanced further such a performance [9, 35]. However, the 1 wt.% PANI-Graphene suspension in 20 cSt silicone oil presents a decisive drawback, if compared to its PANI-WO_3 counterpart. The high leakage current arisen limits the feasible electric field range to about 1.0 kV/mm. So, the maximum efficiency attained may be insufficient for some practical applications. The selection of a silicone oil with higher viscosity, for example 100 cSt, may become an alternative which allows augmenting the ER performance of the 1 wt.% PANI-Graphene suspension. In contrast, it was possible to reach a viscosity increase of almost three orders of magnitude with the 1 wt.% PANI-WO_3 suspension in 20 cSt silicone oil.

Isothermal dynamic shear tests in the linear regime are always associated to a basic rheological characterization of any type of viscoelastic material. They provide very precise information on the material response to small amplitude oscillations, referred to as SAOS, which do not alter its original microstructure. Figures 10A and 10B show frequency sweeps within the linear viscoelastic region, at 25ºC, for the 1 wt.% PANI-Graphene suspensions in 100 and 20 cSt silicone oils, respectively.

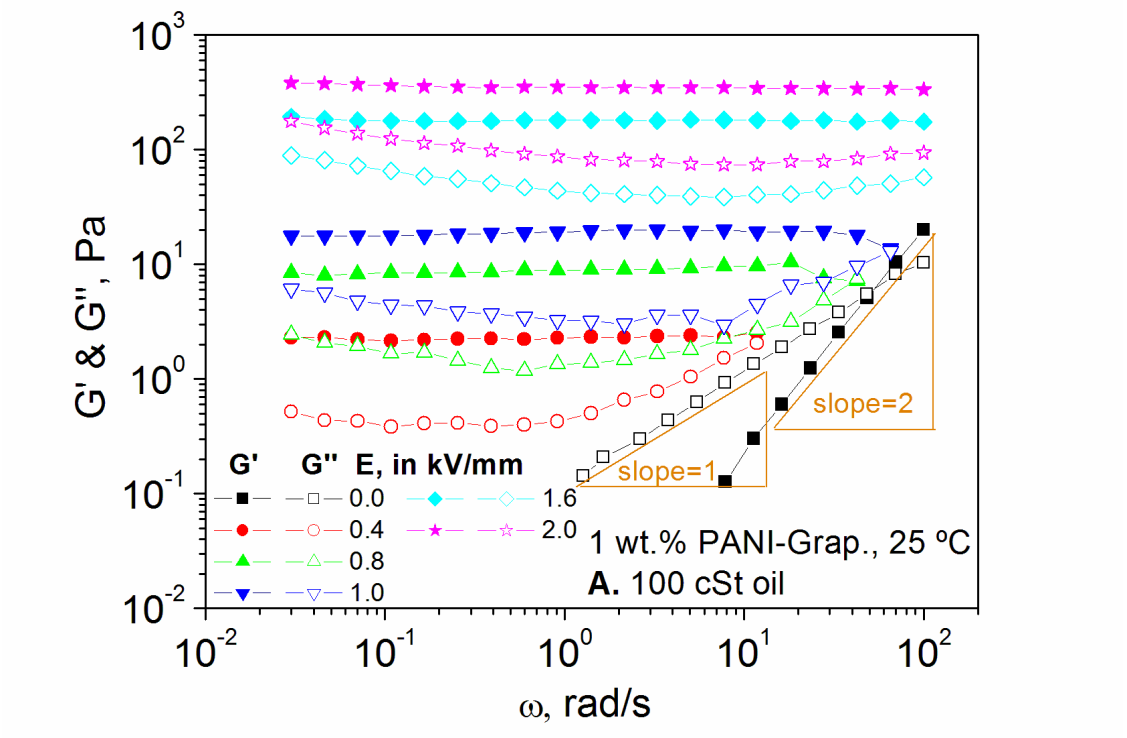

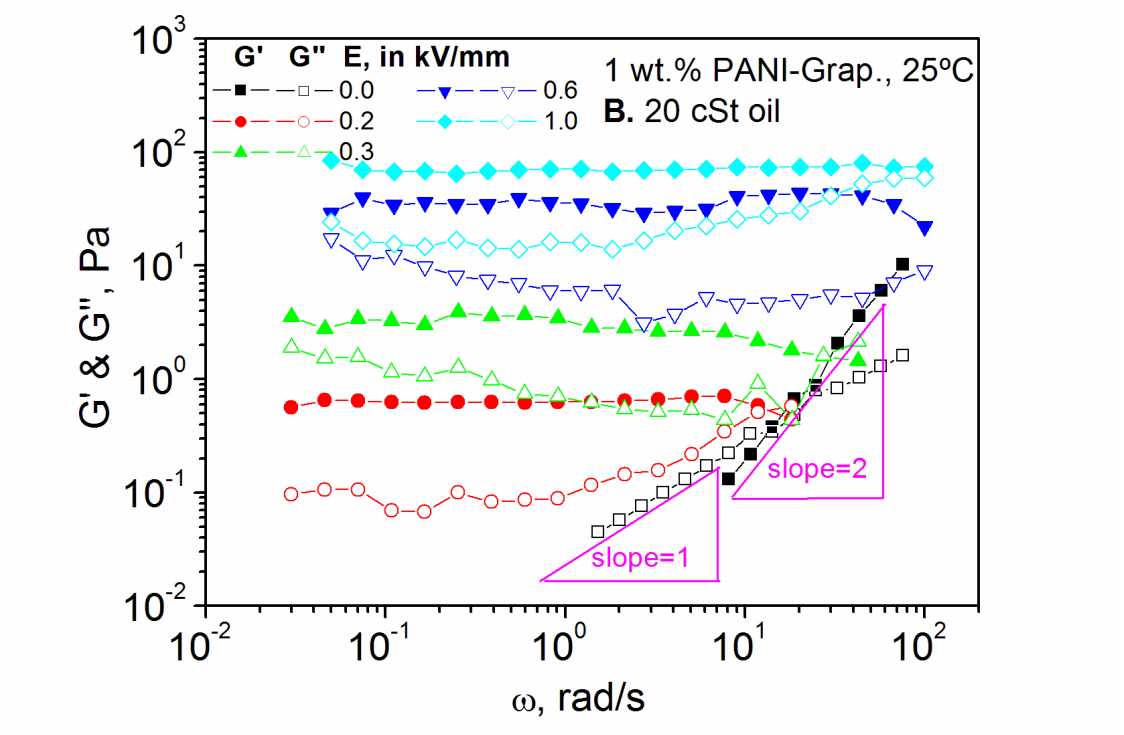

Figure 10. Evolution of the linear elastic (G') and viscous (G'') moduli, at 25ºC, with frequency as a function of the electric field for 1 wt.% PANI-Graphene suspensions in silicone oil with 100 cSt (A) and 20 cSt (B).

In both cases, the rheological behavior without electric field is the usual one for a viscoelastic liquid in the viscous flow region. That is, prevailing viscous behavior, with the elastic and viscous moduli varying as second and first power of the imposed frequency, respectively: $G'(\omega) \sim \omega^2$, $G''(\omega) \sim \omega$. With the application of an electric field, a transition from viscoelastic liquid to gel-like (or solid-like) behavior occurs. Such a behavior is characterized by the elastic modulus being almost insensitive to frequency variations (a well-developed "plateau" region) and a minimum in the viscous modulus, with G'>G'', as seen in Figures 10A and 10B. With increasing the electric field both moduli increase, the minimum in G'' shifts to higher frequencies and the plateau region extends over a wider frequency interval. A simple observation of the evolution of G' with the electric field denotes an important ER effect. In gel-like materials, the value of G' at the frequency when tanδ=G''/G' reaches a minimum, termed "plateau" modulus G_N^0,

represents a measure of the strength of the microstructural network [36]. Again, a higher performance was observed when the 1 wt.% PANI-Graphene suspension was prepared with 100 cSt silicone oil, because it was possible to reach much higher electric fields without detecting excessive leakage current flows. However, no liquid-to-solid transition was observed for electric fields below 0.4 kV/mm. Conversely, when 20 cSt silicone oil was used, the ER effect was noticed at an electric field value as low as 0.2 kV/mm, because a dispersing medium with lower viscosity enables the onset of the columnar structures formation at lower values of the electric driving force.

Fast reversibility of the ER effect upon ceasing the electric field is a must for this type of smart materials. The vast majority of related literature presents, in a greater or lesser extent, a rheological characterization mainly focused on the viscous flow and, sometimes, viscoelastic behavior. However, reversibility is taken for granted and, so, little attention is often paid to this issue. On these grounds, PANI-Graphene suspensions were subjected to the following protocol: a set of viscous flow tests, at 25ºC, at progressively increasing electric fields up to a maximum value, followed by the reverse decreasing ramp down to zero electric field. The results for the 1 wt.% PANI-Graphene suspensions in 100, 50 and 20 cSt silicone oils are shown in Figures 11A to 11C, respectively, in the form of steady shear viscosity curves. The maximum values of electric field applied were 1.6 kV/mm for 100 and 50 cSt silicone oil, and 0.9 kV/mm for 20 cSt silicone oil.

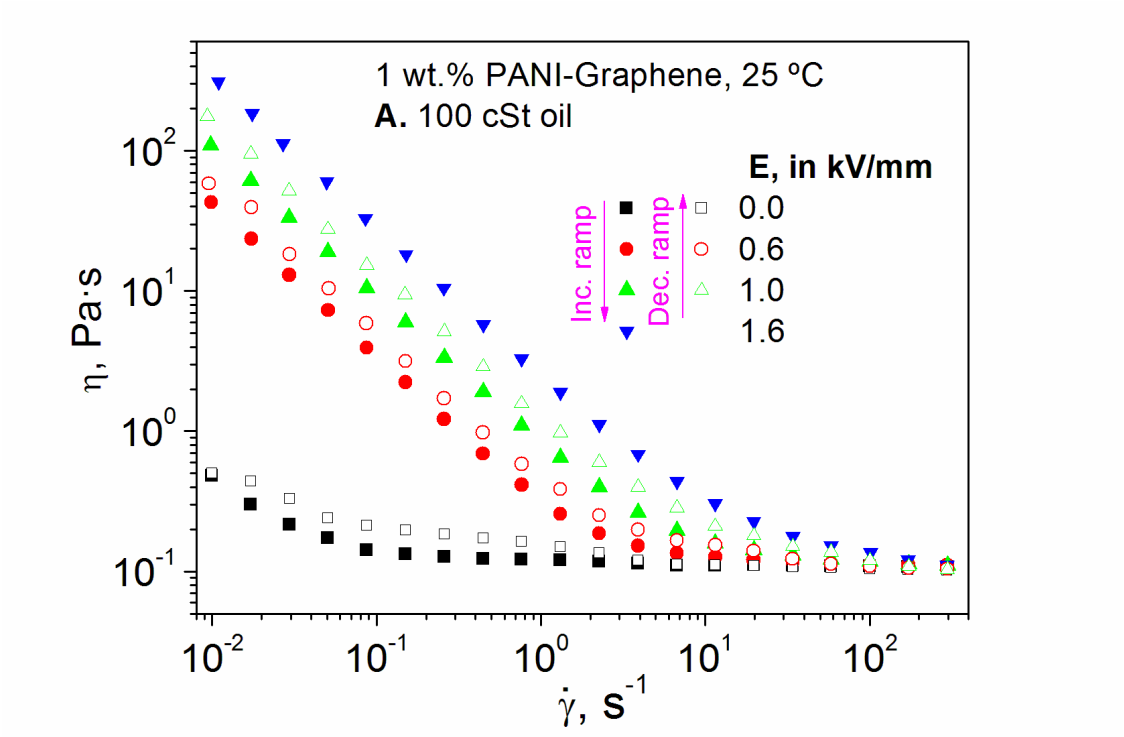
1 wt.% PANI-Graphene, 25 ºC
A. 100 cSt oil
E, in kV/mm
0.0
0.6
1.0
1.6
Inc. ramp
Dec. ramp
η, Pa·s
γ̇, s-1

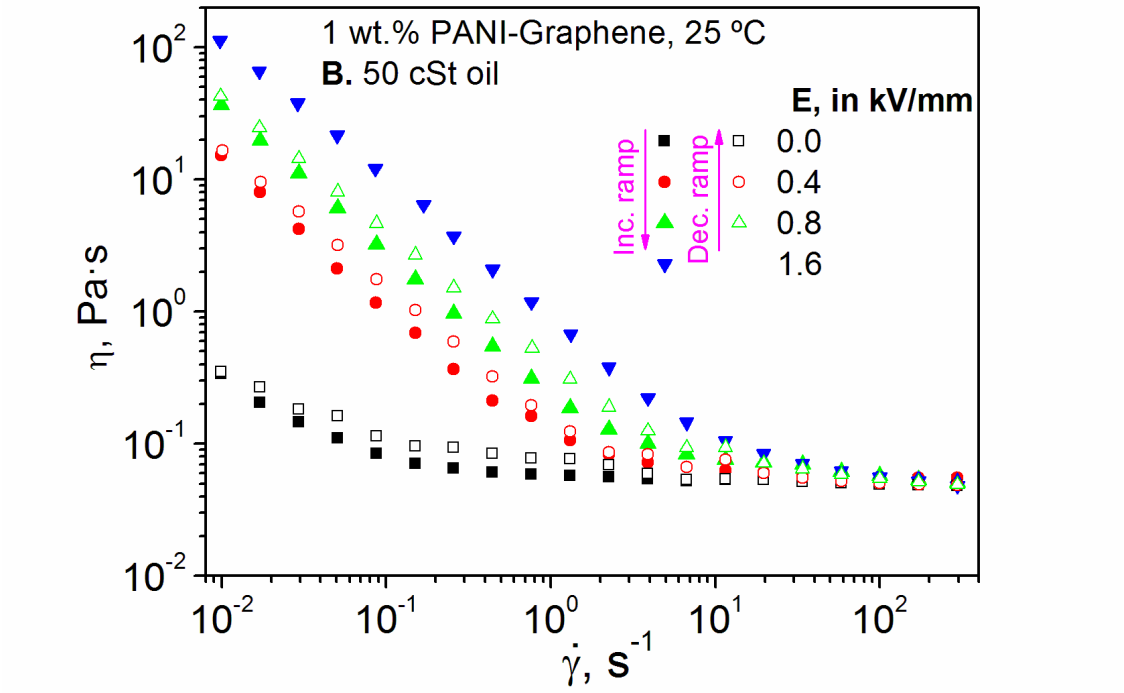
1 wt.% PANI-Graphene, 25 ºC
B. 50 cSt oil
E, in kV/mm
0.0
0.4
0.8
1.6
Inc. ramp
Dec. ramp
η, Pa·s
γ̇, s-1

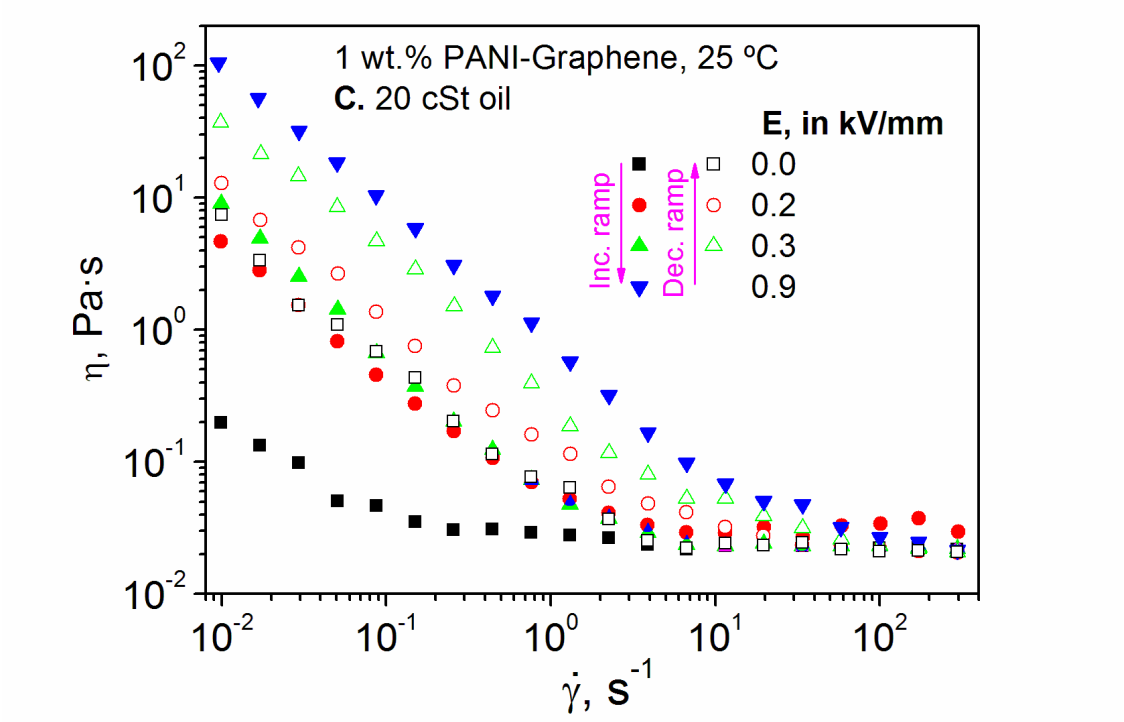

Figure 11. Steady shear viscosity curves, at 25ºC, at selected electric fields applied in a sequence of increasing/decreasing intensities. Tests conducted on 1 wt.% PANI-Graphene suspensions in silicone oil with 100 cSt (A), 50 cSt (B) and 20 cSt (C).

Figures 11A and 11B demonstrate that for the 100 or 50 cSt silicone oil suspensions, although some hysteresis may occur at the highest E values studied, both start and end 0 kV/mm curves almost coincide. Conversely, large hysteresis was noticed when the suspension was prepared with the 20 cSt silicone oil, even at very low E values. Upon completion of a shear rate ramp, disruption of the columnar structures by the hydrodynamic forces must have occurred. Before the following test is run, these structures re-assemble at the extent corresponding to newly electric field set (open and solid symbols should almost coincide, as occurs in Figures 11A and 11B for the most viscous oils). However, Figure 11C evidences that the 1 wt.% PANI-Graphene suspension in 20 cSt silicone oil exhibits higher viscosity than that corresponding to the electric field set. To the best of our knowledge, this effect has not been reported before. Gorodkin et al. [37] found irreversible effects in magnetorheological fluids based on

carbonyl iron particles in silicone oil or water, upon ceasing the magnetic field imposed. This behavior was attributed to the existence of "residual" structures due to non-magnetic interactions provoked by the particle surface chemistry or to residual magnetization. In a similar way, we hypothesize that the PANI-Graphene particle studied partially retains, temporarily, the polarization induced by the electric field previously imposed. So, in silicone oil with low viscosity, the particles are able to re-arrange into more structured alignments than those corresponding to the electric field newly applied. On the contrary, only slightly higher viscosities than expected were observed in 100 or 50 cSt silicone oils, because they offered more resistance to particle orientation and arrangement.

In order to look further into the above phenomenon, a second protocol, also at 25ºC, was established. The electric field was increased up to a set value, and a shear rate ramp was carried out. Subsequently, the electric field was turned off, and shear rate ramps were conducted immediately (0') and after 12 minutes (12' later).

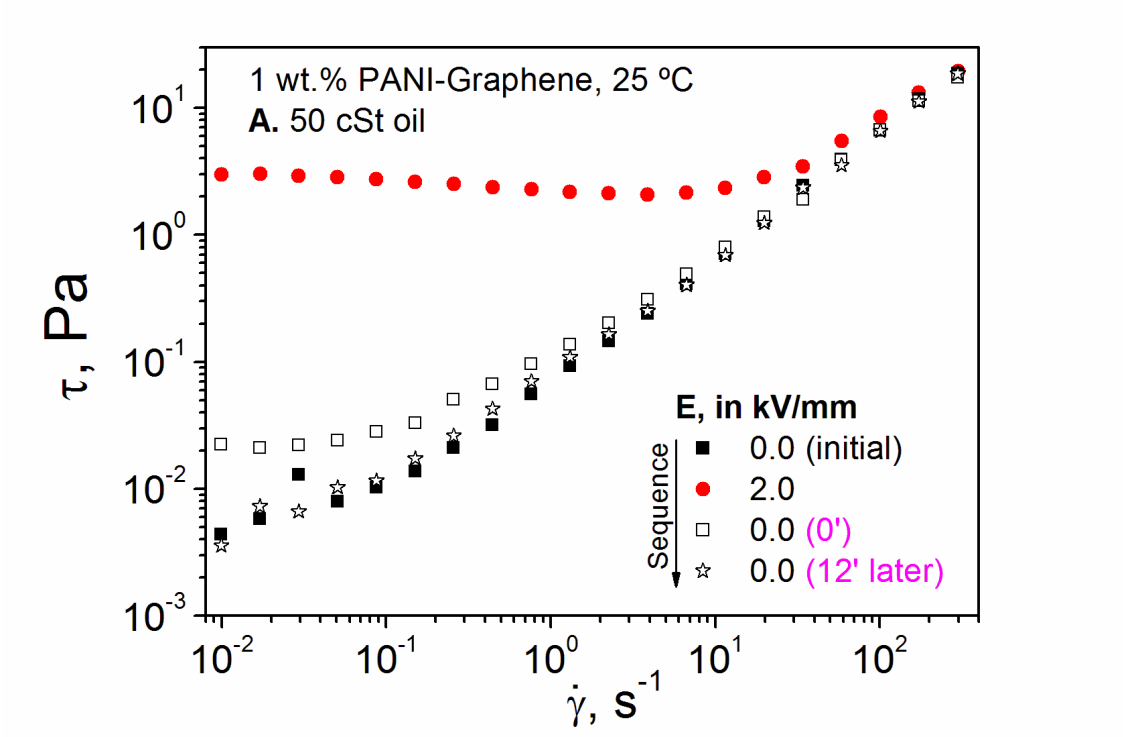

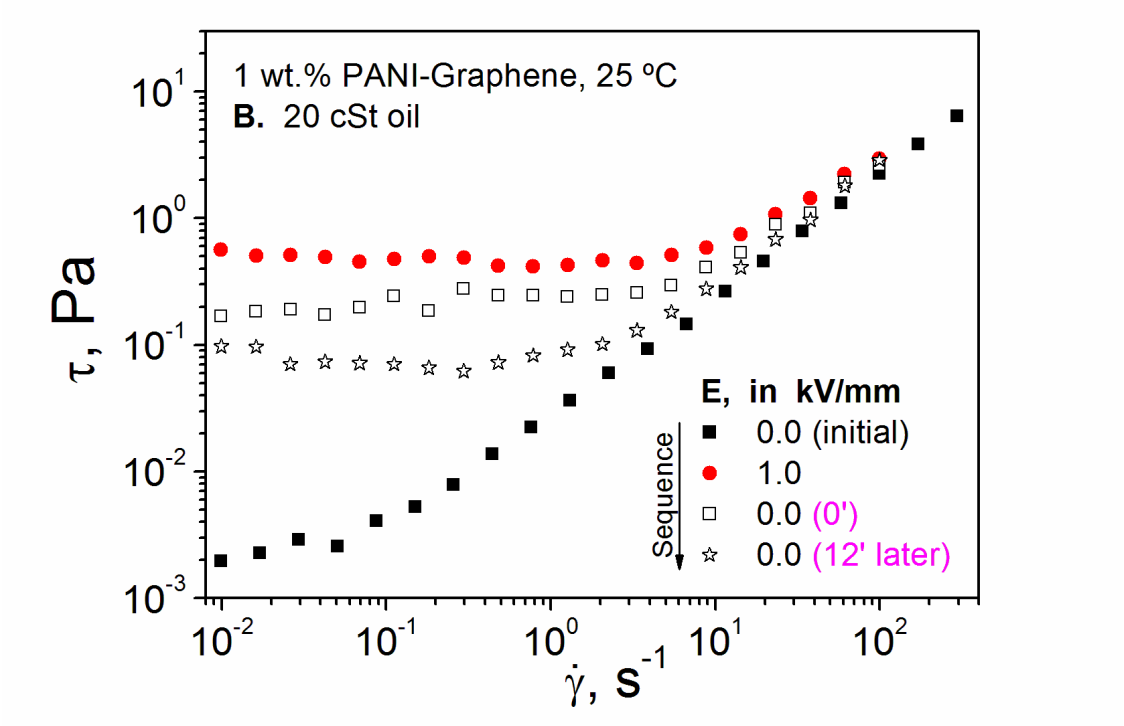

Figure 12. Evolution of the viscous flow behavior, at 25ºC, with the elapsed time upon ceasing an initially set electric field. Tests conducted on 1 wt.% PANI-Graphene suspensions in silicone oil with 50 cSt (A) and 20 cSt (B).

Figures 12A and 12B illustrate the viscous flow behavior under the specified conditions, for the 1 wt.% PANI-Graphene suspensions in 50 and 20 cSt silicone oils, respectively. Little effect of the retained polarization was observed for the 50 cSt silicone oil suspension such that it almost returned to its original state immediately, upon switching off an electric field of 2 kV/mm. As for the 20 cSt, minor removal of the retained polarization was noticed after 12 minutes. PANI was prepared by simple chemical oxidative polymerization of aniline monomer in presence of ammonium persulfate as oxidant and hydrochloric acid as dopant. Thus, in its doped state, PANI presents a high conductivity. As graphene, with very high conductivity, was further incorporated to PANI, the result is a highly conductive hybrid nanocomposite. This was already noticed when the leakage current was evaluated, as previously reported. This result contrasts, for example, with Zhang et al. [3, 11] where graphene oxide, with lower conductivity than

PANI, was used to tune the polymer conductivity. In the present investigation, the PANI-Graphene particles temporarily retain the polarization induced at 1 kV/mm, as a consequence of their high conductivity. Thus, as described above for the 20 cSt silicone oil, disrupted columnar structures at the end of a stress ramp are able to re-assemble prior to the following test even when the electric field is off. This brings about the yield stress observed, even though Newtonian flow behavior was expected.

4. Conclusions

The ER behavior, at 25ºC, of 1 wt.% suspensions of PANI-Graphene or PANI-WO_3 particles in silicone oil with varying viscosities was studied. At such a low concentration, the suspensions showed quasi Newtonian viscous flow behavior in the absence of an electric potential. Conversely, the application of an electric field perpendicular to the shear direction brought about a yield stress, due to the alignment of polarized particles, which increased with the field intensity. At medium shear rate values, before the flow commenced, a minimum in the yield stress arose. Unlike standard viscoplastic fluids, ER suspensions have the capacity to partially re-establish structures broken by shear. The evolution of the steady viscosity with shear rate results from a balance between the hydrodynamic forces which rupture the particles arrangements, and the electrostatic interactions among the polarized particles which tend to re-establish them. In terms of the linear viscoelastic behavior, a transition from viscoelastic liquid to gel-like behavior occurs. Higher values of the "plateau" modulus G_N^0 were observed with the increase of the electric field intensity.

The formation of ER structures consists in two stages: particles electric polarization, which mainly depends on their dielectric constant, and their further assembly into aligned arrays, this latter being strongly influenced by the dispersing medium viscosity. The

viscosity gain relative to the zero field viscosity was higher for the graphene-based particle, and enhanced by the less viscous silicone oil. With regard to the PANI-Graphene suspension, the use of 20 cSt silicone oil brought two major consequences. This medium offered low resistance to particle orientation, yielding a more efficient assembly of polarized particles. This fact, joint to the high conductivity of the PANI-Graphene nanocomposite, explains the high leakage current flows arisen, via tunneling effect between graphene particles, and limits its practical application. Moreover, large viscosity hysteresis was noticed when the suspension was evaluated after the electric field was turned off. We hypothesize that the PANI-Graphene particle studied partially retains, temporarily, the polarization induced by the electric field previously imposed. Thus, in silicone oil with low viscosity, the particles are able to re-arrange into structured alignments even in the absence of electric field. The selection of silicone oil with higher viscosity contributes to re-establish complete reversibility. Further investigation on this issue can result of extreme importance.

5. Acknowledgements

This work was funded by Banco de Santander, through the “Iberoamérica Santander Investigación” Scholarship awarded to Moisés García-Morales and FCT - Portuguese Foundation for Science and Technology, Reference UID/CTM/50025/2013 and FEDER funds through the COMPETE 2020 Programme under the project number POCI-01-0145-FEDER-007688. S. Goswami acknowledges the funding from European Community H2020 program under grant agreement No. 685758 (project 1D-Neon) and A. C. Marques is supported by FCT-MCTES under fellowship SFRH/BD/115173/2016.

Declarations of interest: none

6. References

[1] S. Guragain, B.P. Bastakoti, V. Malgras, K. Nakashima, Y. Yamauchi, Multi-stimuli-responsive polymeric materials, Chem. Eur. J. 21 (2015) 13164 – 13174, doi: 10.1002/chem.201501101.

[2] J.P. Coulter, K.D. Weiss, J.D. Carlson, Engineering applications of electrorheological materials, J. Intell. Mater. Syst. Struct. 4 (1993) 248–259.

[3] W.L Zhang, B.J. Park, H.J. Choi, Colloidal graphene oxide/polyaniline nanocomposite and its electrorheology, Chem. Commun. 46 (2010) 5596–5598.

[4] Y.D. Liu and H.J. Choi, Electrorheological fluids: smart soft matter and characteristics, Soft Matter 8 (2012) 11961-11978.

[5] S.H. Kwon, S.H. Piao, H.J. Choi, Electric Field-Responsive Mesoporous Suspensions: A Review, Nanomaterials 5 (2015) 2249-2267, doi:10.3390/nano5042249.

[6] W.M. Winslow, Induced Fibrillation of Suspensions, J. Appl. Phys. 20 (12) (1949) 1137-1140, doi:10.1063/1.1698285.

[7] H.J. Choi and M.S. Jhon, Electrorheology of polymers and nanocomposites, Soft Matter 5 (2009) 1562-1567.

[8] S. Goswami, T. Brehm, S. Filonovich and M.T. Cidade, Electrorheological properties of polyaniline vanadium oxide nanostructures suspended in silicone oil, Smart Mater. Struct. 23 (2014) 105012, doi:10.1088/0964-1726/23/10/105012.

[9] S. Goswami, P. Gonçalves, M.T. Cidade, Electrorheological behavior of suspensions of camphorsulfonic acid (CSA) doped polyaniline nanofibers in silicone oil, Phys. Scr. 92 (2017) 075801, https://doi.org/10.1088/1402-4896/aa70f7.

[10] Y.D. Liu and H.J. Choi, Electrorheological response of polyaniline and its hybrids, Chem. Pap. 67 (2013) 849-859.

[11] W.L. Zhang, Y.D. Liu, H.J. Choi, Fabrication of semiconducting graphene oxide/polyaniline composite particles and their electrorheological response under an applied electric field, Carbon 50 (2012) 290 – 296, doi:10.1016/j.carbon.2011.08.049.

[12] K.Y. Shin, S. Lee, S. Hong, J. Jang, Graphene size control via a mechanochemical method and electroresponsive properties, ACS Appl. Mat. Interfaces 6(8) (2014) 5531–5537, http://dx.doi.org/10.1021/am405930k.

[13] J.B. Yin, X.X. Wang, R.T. Chang, X.P. Zhao, Polyaniline decorated graphene sheet suspension with enhanced electrorheology, Soft. Matter. 8(2) (2012a) 294–297.

[14] J.B. Yin, Y.J. Shui, R.T. Chang, X.P. Zhao, Graphene-supported carbonaceous dielectric sheets and their electrorheology, Carbon 50 (2012b) 5247 –5255.

[15] S. Deb, Novel electro-photographic system, Applied Optoelectronics 3 (1969) 192–193.

[16] R.R. Kharade, S.R. Mane, R.M. Mane, P.S. Patil, P.N. Bhosale, Synthesis and characterization of chemically grown electrochromic tungsten oxide, J. Sol–Gel Sci. Technol. 56 (2010) 177-183.

[17] C.G. Granqvist, Hand Book of Inorganic Electrochromic Materials, first ed., Amsterdam, Elsevier, ISBN: 9780080532905, 1995.

[18] S. Yoon, C. Jo, S.Y. Noh, C.W. Lee, J.H. Song, J. Lee, Development of a high-performance anode for lithium ion batteries using novel ordered mesoporous tungsten oxide materials with high electrical conductivity, Phys. Chem. Chem. Phys. 13(23) (2011) 11060-11066.

[19] W.J. Li and Z.W. Fu, Nanostructured WO_3 thin film as a new anode material for lithium-ion batteries, Appl. Surf. Sci. 256 (2010) 2447–2452, http://dx.doi.org/10.1016/j.apsusc.2009.10.085.

[20] B.X. Zou, X.X. Liu, D. Diamond, K.T. Lau, Electrochemical synthesis of WO_3/PANI composite for electrocatalytic reduction of iodate, Electrochim. Acta 55 (2010) 3915–3920.

[21] H.G. Wei, X.R. Yan, S.J. Wu, Z.P. Luo, S.Y. Wei, Z.H. Guo, Electropolymerized polyaniline stabilized tungsten oxide nanocomposite films: electrochromic behavior and electrochemical energy storage, J. Phys. Chem. C 116 (2012) 25052–25064.

[22] G.C. Barber, Q.Y. Jiang, Q. Zou, and W. Carlson. Development of a Laboratory Test Device for Electrorheological Fluids in Hydrostatic Lubrication, Tribotest Journal, 11 (2005) 185.

[23] J. Lin, Z. Peng, Y. Liu, F. Ruiz-Zepeda, R. Ye, E.L.G. Samuel, M.J. Yacaman, B. I. Yakobson, J.M. Tour, Laser-induced porous graphene films from commercial polymers, Nat. Commun. 5 (2014) 5714.

[24] L. Santos, J.P. Neto, A. Crespo, D. Nunes, N. Costa, I.M. Fonseca, P. Barquinha, L. Pereira, J. Silva, R. Martins, E. Fortunato, WO_3 Nanoparticle-Based Conformable pH Sensor, ACS Appl. Mater. Interfaces 6 (2014) 12226−12234.

[25] G.F. Cai, J. P. Tu, D. Zhou, J. H. Zhang, X. L. Wang, C. D. Gu, Dual electrochromic film based on WO_3/polyaniline core/shell nanowire array, Sol. Energy Mater. Sol. Cells 122 (2014) 51–58.

[26] C. Janaky, N. R. Tacconi, W. Chanmanee, K. Rajeshwar, Electrodeposited Polyaniline in a Nanoporous WO3 Matrix: An Organic/Inorganic Hybrid Exhibiting Both p- and n-Type Photoelectrochemical Activity, J. Phys. Chem. C 116 (2012) 4234−4242.

[27] S. Goswami, S. Nandy, J. Deuermeier, A. C. Marques, D. Nunes, S. P. Patole, P. M. F. J. Costa, R. Martins, E. Fortunato, Green Nanotechnology from Waste Carbon–Polyaniline Composite: Generation of Wavelength-Independent Multiband Photoluminescence for Sensitive Ion Detection, Adv. Sustainable Syst. 2 (1) (2018) 1700137.

[28] S. H. Domingues, R. V. Salvatierra, M. M. Oliveira, A. J. G. Zarbin, Transparent and conductive thin films of graphene/polyaniline nanocomposites prepared through interfacial polymerization, Chem. Commun. 47 (2011) 2592–2594.

[29] X. Chen, F. Meng, Z. Zhou, X. Tian, L. Shan, S. Zhu, X. Xu, M. Jiang, L. Wang, D. Hui, Y. Wang, J. Lu, J. Gou, One-step synthesis of graphene/polyaniline hybrids by in situ intercalation polymerization and their electromagnetic properties, Nanoscale 6 (2014) 8140–8148.

[30] H.A. Barnes, Viscosity, University of Wales, Institute of Non-Newtonian Fluid Mechanics, Aberystwyth, Wales, 2002.

[31] Y.P. Seo, H.J. Choi, Y. Seo, Analysis of the flow behavior of electrorheological fluids with the aligned structure reformation, Polymer, 52 (2011) 5695.

[32] V. Pavlinek, P. Saha, T. Kitano, T. Tanegashima, Influence of the Electric Field on the Electrorheological Behaviour of Cellulose Suspensions in Silicone Oils, Appl. Rheol. 9 (1999) 64.

[33] R. Patra, S. Suin, D. Mandal, B.B. Khatua, Sequential mixing as effective method in the reduction of percolation threshold of multiwall carbon nanotube in poly(methyl methacrylate)/high-density poly(ethylene)/MWCNT nanocomposites, J. Appl. Polym. Sci. 131 (10) (2014) 40235.

[34] A. Lengalova, V. Pavlinek, P. Saha, J. Stejskal, T. Kitano, O. Quadrat, The effect of dielectric properties on the electrorheology of suspensions of silica particles coated with polyaniline, Physica A 321 (2003) 411 – 424.

[35] T. Brehm, G. Pereira, C.R. Leal, C. Gonçalves, J.P. Borges, M.T. Cidade, Electrorheological characterization of dispersions in silicone oil of encapsulated liquid crystal 4-n-penthyl-4′-cyanobiphenyl in polyvinyl alcohol and in silica, Phys. Scr. 90 (2015), 035802.

[36] R. Sánchez, G. Alonso, C. Valencia, J.M. Franco, Rheological and TGA study of acylated chitosan gel-like dispersions in castor oil: Influence of acyl substituent and acylation protocol, Chem. Eng. Res. Des. 100 (2015) 170–178.

[37] S. Gorodkin, R. James, W. Kordonski, Irreversible effects in magnetorheological fluids, J. Intell. Mater. Syst. Struct. 22 (2011) 1749–1754.